Int. J. Environ. Sci. Technol. (2014) 11:449–460
DOI 10.1007/s13762-013-0219-y

ORIGINAL PAPER

Commercial steel wool for reduction of hexavalent chromium in wastewater: batch kinetic studies and rate model

P. Mitra · P. Banerjee · D. Sarkar · S. Chakrabarti

Received: 14 May 2012 / Revised: 14 January 2013 / Accepted: 23 February 2013 / Published online: 20 March 2013

Abstract The present study aims at searching the potential of commercial grade steel wool in reducing hexavalent chromium in aqueous phase under batch mode. About 30 % of the initial hexavalent chromium was found to reduce within 2 h at a pH of 3. However, on testing the combined effects of different process parameters, namely the solution pH, wool loading, etc., the optimum batch parametric condition has been fixed. A moving boundary type kinetic model, which takes into account the effect of passivation along with the direct reduction mechanism to simulate the gross uptake profile of Cr(VI) from the bulk solution is proposed. The effective pore diffusivity of Cr(VI) in commercial steel wool was determined by a suitable global optimization technique. Additionally, the model is also capable to simulate the decline of active external surface area of the wool caused by passivation with time. A good match of the experimental data and model-simulated transient bulk concentration of Cr(VI) (under optimum parametric condition only) establishes the general validity of the proposed model.

Keywords Batch study · Heavy metal · Kinetic model · Passivation · Zero-valent iron

Introduction

The metal shavings resulting from peeling away metal using lathes were found to be an interesting waste during the 1990s. At first, this swarf was used to polish metal surfaces. Since the mass of metal strings resembled wool or fiber, it was named as steel wool though it is not spun as a fiber. Instead, steel wool is produced by a process known as drawing. These steel wool pads are used for a variety of purposes, primarily as an abrasive material, sometimes replacing sandpaper (Özer et al. 1997). Commercial steel wool is available in the market in a variety of grades that stand for the roughness or thicknesses, ranging from coarse to extra fine. The thicker the strand of wool, the more abrasive it is against the surface.

Steel wool obtained out of low-carbon steel typically has high surface area to volume ratio (Kogel et al. 2006). In the processes where zero-valent iron (ZVI) particles are used for chemical reduction with a purpose of environmental remediation, steel wool can be a very suitable candidate. One such case is reduction of hexavalent chromium present in wastewater to the trivalent state. Chromium has two common stable oxidation states in the environment, hexavalent chromium [Cr(VI)] and trivalent chromium [Cr(III)]. Cr(VI) is a known carcinogen and highly mobile so that it neither precipitates nor gets adsorbed readily (Katz and Salem 1992; Cheryl and Susan 2000). Cr(VI) normally exists as chromate, [CrO_4^{2-}] or [$HCrO_4^-$] and dichromate [$Cr_2O_7^{2-}$]. Cr(III), on the other hand is less toxic, non-carcinogen and a desirable micronutrient that can be separated as sparingly soluble precipitates.

A number of physical and chemical techniques have been reported for the removal of chromium from wastewater and groundwater. Adsorption with suitable adsorbents (Bowers and Huang 1980), solvent-extraction and membrane separation processes like reverse osmosis or separation by liquid membrane (Kulkarni et al. 2007) are among the physical methods. The chemical methods use a suitable reducing agent. The Cr(III) obtained by reduction, may be precipitated and separated out by changing pH of

P. Mitra · P. Banerjee · D. Sarkar · S. Chakrabarti (✉)
Department of Chemical Engineering, University of Calcutta, Kolkata 700 009, India
e-mail: sampac.2008@gmail.com

the medium to the alkaline range. Agrawal et al. (2006) reviewed the various techniques of treatment of effluents containing hexavalent chromium emanating from the leather tanning and electroplating industries. They exhaustively described and compared most of the possible methodologies like solvent extraction, reduction-precipitation, adsorption, membrane separation, ion exchange and biological reduction. Besides requirement of excess chemicals to insure complete conversion of Cr(VI), formation of sludge is a major problem often faced in the above conventional methods.

Two other methods of Cr(VI) remediation that have shown considerable potential are photocatalytic reduction with semiconductors (Ku and Jung 2001) and use of ZVI. Because of the low cost of reductant and ease of operations, ZVI has received great attention as a reducing agent for Cr(VI).

The technology of remediation of contaminated groundwater using permeable-reactive redox barriers (PRBs) is based on metallic iron (Puls et al. 1999; Blowes et al. 2000; Wilkin et al. 2005). Redox-active solids used in PRBs like ZVI, promote rapid removal of redox-sensitive contaminants, such as Cr(VI), mainly by adsorption and reductive precipitation. For the treatment of industrial wastewater granular iron particles, iron filings or steel wool are practically feasible options for reduction of Cr(VI) due to their large surface area. Wang et al. (2010) used iron-encapsulated alginate beads and observed that the reduction of Cr(VI) was strongly dependent on the solution pH. Kinetic data followed the second-order rate equation. Rivero-Huguet and Marshall (2009) prepared a series of nano-sized bi-metallic and tri-metallic iron particles doped with one or more of the metals like Pd, Ag, Cu, Zn, Co, Mg, Ni, Al, Si and evaluated them for reduction of Cr(VI) leached out by surfactant solutions from contaminated soils. Presence of a metal-dopant was found to enhance the activity of the iron particles.

Reduction of Cr(VI) with Fe(0) (ZVI) occurs through the reaction:

$$2\,Fe^{0} + Cr_2O^{2-}_{7(aq)} + 14\,H^{+} \rightarrow 2\,Fe^{3+}_{(aq)} + 2\,Cr^{3+}_{(aq)} + 7\,H_2O \quad (1)$$

In addition to the above reaction, a simultaneous passivation reaction occurs during ZVI–Cr(VI) contact in acidic medium. The decrease in the rate of reduction with time observed by many researchers might be due to passivation of the iron surface or the active reaction sites (Williams and Scherer 2001; Melitas et al. 2001). This passivation reaction converts metallic iron to a composite oxyhydroxide of iron(III)–chromium(III) with low electrical conductivity that prevents passage of electrons from Fe(0) to Cr(VI). Similar passivation has been reported during reduction by magnetite also (He and Traina 2005).

After reduction, the resulting trivalent chromium in aqueous solution undergoes co-precipitation with Fe(III) to form Fe(III), $Cr(OH)_{3(s)}$ (Sass and Rai 1987; Eary and Rai 1988). Reduction of Cr(VI) may also be done by Fe(II)-bearing solid phases or dissolved Fe^{2+} followed by sorption of dissolved Cr(VI) and Cr(III) on Fe(II/III) oxyhydroxides. Coelho et al. (2008) studied its role of magnetite on the reduction of Cr(VI) in conjugation with ZVI, although magnetite may be a product for the parallel passivation reaction. The extent and rate of Cr(VI) removal by ZVI have been explored extensively in laboratory (Gould 1982; Cantrell et al. 1995), in column (Blowes et al. 2000) and in field demonstrations (Puls et al. 1999). The results of these studies indicate that the rate of Cr(VI) removal is sufficiently rapid for groundwater remediation using permeable-reactive barriers. Özer et al. (1997) used steel wool for reduction of hexavalent chromium in a continuous column; El-Shazly et al. (2005) used scrap iron for the same purpose.

In one of our previous works, we had employed electrolytic grade iron dust for reducing hexavalent chromium. There we had reported different aspects of the batch reaction with ZVI in the form of iron dust and potassium dichromate solution (Dutta et al. 2010). In case of steel wool, iron filings or scrap iron, it is difficult to determine the geometry or surface area of such irregular-shaped reductant accurately, and therefore it is nearly impossible to propose any rate model for the surface-reduction process since the rate equation explicitly contains transient active surface area. In our recent work (Mitra et al. 2011), we used thin rectangular mild steel plates for the reduction of hexavalent chromium in aqueous solution where the substrate had a known and unchanging surface area. We collected the time–concentration data in batch experiments varying the initial solution concentrations and pH. A kinetic model was proposed for the reduction process considering the simultaneous passivation reaction as well and the same was validated using the experimental data. This approach has not been taken before in any other available work.

The present research is aimed at the exploration of the efficacy of steel wool for reduction of hexavalent chromium. Neither of the works of Özer et al. (1997) and El-Shazly et al. (2005) described the kinetics of the batch process in detail. In this work, we have reported reduction of hexavalent chromium as present in aqueous potassium dichromate solution using steel wool in batches. The process parameters studied are loading of steel wool, pH, initial concentration of hexavalent chromium, temperature and presence of salt. A kinetic model has been proposed in this case also and the same was validated using the

experimental data. In this context, it should be mentioned that the values of the rate constants for reduction (k_1) and passivation (k_2) as well as α (as in Eq. 11) have been taken from our work with the steel plate and the same are applied in this case. The rationale for taking the values has been given under the "Measurement of process parameters".

The research work was carried out in the Department of Chemical Engineering, University of Calcutta, Kolkata, India during the months of March to July in the year 2011.

Model formulation

The traditional models regarding the Cr(VI)–Fe(0) reaction kinetics were approached using the simplified concepts of homogeneous reactions. For example, works of Gould (1982) and Blowes et al. (1996) first revealed a 0.5 order kinetics with respect to the bulk Cr(VI) concentration. However, the actual reaction system is heterogeneous, and therefore, the corresponding kinetic approach is likely to reflect the actual picture. Recently, Fiúza et al. (2010) have proposed a shrinking particle type model of 2/3rd order kinetics assuming the rate to be proportional to the available iron surface area and to the bulk volume, though the transient reduction of external surface area of Fe(0) was neglected. On the other hand, Song et al. (2005) proposed a simple first order kinetics to describe the effect of sand in Cr(VI)/Fe(0) kinetics. Their model is once again of the complexities of heterogeneous system. A lot of works have been reported on the modeling of solid–fluid non-catalytic reactions over decades. A general model based on local volume approach, which is capable of handling non-linear kinetics and change of porous structure during conversion, was proposed by Gómez-Barea and Ollero (2006). Another finite volume-based, numerical model (Patisson et al. 1998) is also available in literature. The model is claimed to simulate the thermal behavior of porous pellets in addition to kinetics.

A detailed literature review indicates that the available models of solid–fluid non-catalytic reaction can incorporate a wide variety of complexities like the deformation of porous structure, effects of inert gas, reversibility of a chemical reaction, etc. No attempts were made to incorporate the transient blockage of external solid surface area due to passivation via a competitive parallel kinetics, like in Cr(VI)/Fe(0) system. Therefore, the present model may be viewed as a semi-empirical extension of standard progressive conversion model (PCM) (Levenspeil 1998) in cylindrical geometry, in order to accommodate the phenomenon of external surface reduction of the solid due to passivation.

In the present model, we have explicitly considered the uptake of Cr(VI) by ZVI via passivation route in addition to the normal uptake of the same by primary reduction route via redox reaction. The details of a similar kinetic model for mild steel plate primarily containing ZVI has been described elsewhere (Mitra et al. 2011). However, in the previous work (Mitra et al. 2011), the system geometry was devoid of any curvature effect, since thin rectangular plates with known dimensions were chosen as a source of ZVI. The previous work was taken up with a sole objective to determine only the kinetic parameters of the Cr(VI)/Fe(0) reaction system. In the present study, attempt has been made to incorporate those kinetic parameters in a moving boundary type model to describe the process of chromate reduction by commercial steel wool, which mostly comprises ZVI with a little bit of impurity. The assumptions of the proposed model are as under:

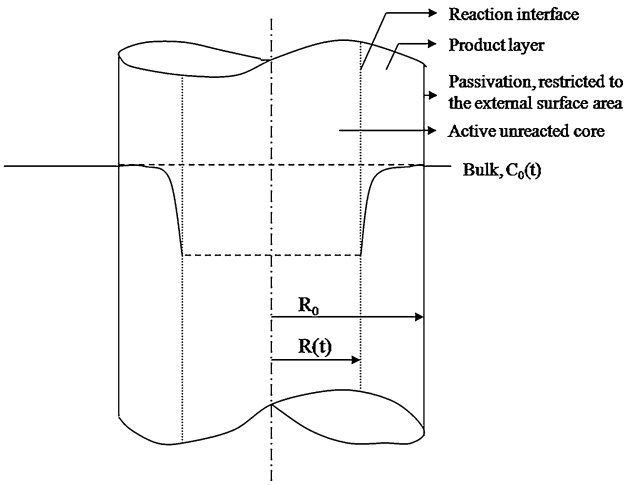

Fig. 1 Qualitative concentration profile of Cr(VI) in steel wool according to the proposed model

1. The whole mass of steel wool is considered to be equivalent to a single long cylinder of finite length with no end effects.
2. Pseudo-steady diffusion of Cr(VI) through the cylindrical shell of the wool (which is in turn the product layer). The physical picture of the model is as described in Fig. 1.
3. Liquid-side film mass transfer resistance is negligibly small (because of vigorous shaking).
4. The product layer thickness is the same as the thickness of Fe(0) layer consumed, i.e., the effective change of steel wool volume has been neglected. This alternatively indicates that the product layer is formed by primary reduction route only when the thickness of the layer formed by passivation route is comparatively much smaller (Mitra et al. 2011).
5. Passivation takes place only on the external surface of the wool strand.

Considering a single strand of steel wool to be a perfect cylinder with negligible end effects (assumption 1), the

pseudo-steady state diffusion equation of Cr(VI) through the product layer that is spanned in the radial domain $r \Rightarrow [R(t), R_0]$ becomes

$$\frac{1}{r}\frac{\mathrm{d}}{\mathrm{d}r}\left(rD\frac{\mathrm{d}C}{\mathrm{d}r}\right) = 0 \tag{1}$$

The appropriate boundary conditions are

(i) at $r = R_0$, $C = C_0(t)$
(ii) at $r = R(t)$, $D\frac{\mathrm{d}C}{\mathrm{d}r} = -R_{\mathrm{Cr(VI)}}\big|_1$

where $R_{\mathrm{Cr(VI)}}\big|_1$ represents the uptake rate of Cr(VI) via the primary redox reaction route (marked as route 1 in (Mitra et al. 2011) per unit surface area of the interface between the product layer and active unreacted core (as shown in Fig. 1). In our previous work on steel plate (Mitra et al. 2011), the same uptake rate was found to be of the following form

$$\left(-\frac{\mathrm{d}C}{\mathrm{d}t}\right)_1 = k_1 A(t) C(t)^{\frac{2}{3}} \tag{2}$$

Accordingly $R_{\mathrm{Cr(VI)}}\big|_1$ can be expressed in terms of k_1 as

$$-R_{\mathrm{Cr(VI)}}\big|_1 = \frac{V(t)}{A(t)}\left(-\frac{\mathrm{d}C}{\mathrm{d}t}\right)_1 = k_1 C(t)^{\frac{2}{3}} V(t) \tag{3}$$

where $V(t)$ is the volume of the active unreacted core, so $V(t) = \pi R(t)^2 L$. The simple analytical solution of Eq. (1), which represents the concentration profile in the product layer, becomes

$$C(t) = P \ln r + Q \tag{4}$$

where P and Q are the constants of integration. Using the boundary conditions and Eq. (3), the simultaneous equations for solving P and Q are as constituted

$$C_0(t) = P \ln R_0 + Q \tag{5}$$

and

$$\frac{DP}{R(t)} = k_1 [P \ln R(t) + Q]^{\frac{2}{3}} \pi R(t)^2 L \tag{6}$$

Equations 5 and 6 clearly indicates that P and Q are time-dependent functions, i.e., $P = P(t)$ and $Q = Q(t)$. Considering the shrinkage rate of the active core from the perspective of assumption 6, the governing equation representing the transient variation of $R(t)$ becomes

$$-\frac{\mathrm{d}}{\mathrm{d}t}[\pi R(t)^2 L \rho \varphi_C] = D\frac{\mathrm{d}C}{\mathrm{d}r}\bigg|_{r=R(t)} 2\pi R(t) L$$
$$\Rightarrow -R\frac{\mathrm{d}R}{\mathrm{d}t} = \frac{DP(t)}{\rho \varphi_C}$$

Integrating

$$R(t) = \sqrt{R_0^2 - \int_0^t \frac{DP(t)}{\rho \varphi_C}\mathrm{d}t} \tag{7}$$

On the other hand, for the external surface of the steel wool, the total Cr(VI) uptake rate remains the same as that of our previous work (Mitra et al. 2011), which is

$$-\frac{\mathrm{d}C_0(t)}{\mathrm{d}t} = \left(-\frac{\mathrm{d}C_0(t)}{\mathrm{d}t}\right)_1 + \left(-\frac{\mathrm{d}C_0(t)}{\mathrm{d}t}\right)_2 = k_1 C_0(t)^{\frac{2}{3}} A(t) + k_2 A(t) C_0(t) \tag{8}$$

The first term on the right-hand side essentially represents the part of Cr(VI) uptake, which diffuses through the wool, whereas the second term represents the uptake via passivation route, the effect of which is restricted over the external surface only. Accordingly,

$$k_1 C_0(t)^{\frac{2}{3}} = \frac{DP(t)}{R_0 \pi R(t)^2 L} \tag{9}$$

Combining Eq. (9) with Eq. (8), the final form of the total uptake rate becomes

$$-\frac{\mathrm{d}C_0(t)}{\mathrm{d}t} = \frac{DP(t)}{R_0 \pi R(t)^2 L} A(t) + k_2 A(t) C_0(t) \tag{10}$$

In addition to the Cr(VI) uptake rate, the rate of reduction of the active external surface area also remains unaltered as previous, hence

$$-\frac{\mathrm{d}A(t)}{\mathrm{d}t} = \alpha k_2 A(t) C_0(t) \tag{11}$$

In formulating Eq. (11), it is assumed that the passivation route of Cr(VI) uptake only is responsible for the external area blockage and subsequently the corresponding rate becomes proportional to the rate of Cr(VI) uptake via the passivation route. Introducing the following dimensionless variables

$$C_0^* = \frac{C_0(t)}{C_{0,\mathrm{in}}},\ t^* = \frac{Dt}{R_0^2},\ A^* = \frac{A(t)}{A_0},\ r^* = \frac{R(t)}{R_0},\ P^* = \frac{P(t)}{C_{0,\mathrm{in}}} \text{ and } Q^* = \frac{Q(t)}{C_{0,\mathrm{in}}}$$

Equations (5)–(7), (10) and (11) can be transformed into the following dimensionless forms

$$C_0^*(t^*) = P^*(t^*) \ln R_0 + Q^*(t^*) \tag{12}$$

$$\frac{P^*(t^*)}{r^*(t^*)} = K_1^* [P^*(t^*) \ln\{r^*(t^*) R_0\} + Q^*(t^*)]^{\frac{2}{3}} r^*(t^*)^2 L^* \tag{13}$$

$$r^*(t^*) = \sqrt{1 - \int_0^{t^*} \frac{P^*(t^*)}{\rho^* \varphi_C}\mathrm{d}t^*} \tag{14}$$

$$-\frac{\mathrm{d}C_0^*(t^*)}{\mathrm{d}t^*} = \frac{P^*(t^*) A^*(t^*) A_0^*}{r^*(t^*)^2 L^*} + K_2^* A^*(t^*) C_0^*(t^*) \tag{15}$$

and

$$-\frac{\mathrm{d}A^*(t^*)}{\mathrm{d}t^*} = K_2^* \alpha^* A^*(t^*) C_0^*(t^*) \tag{16}$$

where $K_1^* = \frac{\pi k_1 R_0^4}{D} C_{0,\text{in}}^{-1/3}$, $L^* = \frac{L}{R_0}$, $\rho^* = \frac{\rho}{C_{0,\text{in}}}$, $A_0^* = \frac{A_0}{\pi R_0^2}$, $V(t)$ and $\alpha^* = \frac{\alpha C_{0,in}}{A_0}$. Equations (12)–(16) can be solved simultaneously by a suitable numerical technique to obtain the transient bulk concentration profile, penetration and active surface area dynamics provided the different model parameters, namely $\rho, R_0, L, A_0, k_1, k_2, \alpha, \varphi_C$ and D are known a priori.

Materials and methods

Materials

Commercial steel wool has been procured from local market. It was washed with acetone and dilute acid. After that it was heat-treated in a muffle furnace at 400 °C to drive out the organic impurities and preserved in a dessicator to prevent atmospheric hydration. EDX data (not shown) show that this ready-to-use steel wool contains mainly iron and oxygen and a small amount of carbon. Laboratory reagent grade potassium dichromate, concentrated sulfuric acid and sodium hydroxide were procured from SRL Chemicals, India. Freshly prepared double distilled water was used for preparing solutions. pH of the solution was measured with digital pH meter (Eutech Instruments waterproof pH Testr 20).

Analytical methods

The residual concentration of dichromate in solution was analyzed using a UV–vis spectrophotometer (Shimadzu UV-160A, Kyoto, Japan) at 349 nm in a 1-cm quartz cell (Botta et al. 1999; Navio et al. 1999; Goeringer et al. 2001) against a standard linear ($R^2 = 0.99$) calibration curve within the concentration range of 0–125 mg L^{-1}.

Both unreacted and reacted steel wool strands were pictured by scanning electron micrograph (SEM) (model LEO S440, Germany) to analyze their surface morphology size and state of aggregation. Energy dispersive spectrometry (EDS, Oxford Link Isis, UK) coupled with the SEM was used to investigate the elements present in the particles.

Experimental procedure

The reaction of dichromate in solution with steel wool was carried out in stoppered borosilicate glass bottles. Measured volumes of the dichromate solution (50 mL) of requisite concentration were taken in each bottle, and the pHs of the solutions were adjusted by adding dilute sodium hydroxide (NaOH) and hydrochloric acid (HCl) solution. The weighed quantity of steel wool was added, and the bottle was placed in a constant-temperature (for majority of the experiments, the temperature was maintained at 31 °C) shaker bath for adequate mixing. The bottles were taken out after predetermined time intervals, and 1–2 drops of alkali solution was added to make pH of the solution alkaline (about 11). A greenish brown precipitate of the mixed hydroxide of Fe(III) and Cr(III) separated out. The solution was filtered (Whatmann grade 2 filter paper) and the supernatant liquid was analyzed for the residual Cr(VI) content. Separate sets were used for monitoring the concentrations at different times to avoid errors resulting from interference during sampling and also from changes in the liquid volume in a batch. Each experiment was repeated at least twice, and the standard deviation was within ±5 %.

Measurement of model parameters

The experimental validation of the proposed model involves the evaluation of different process parameters, viz., $\rho, R_0, L, A_0, k_1, k_2, \alpha, \phi_C$ and D. Values of these

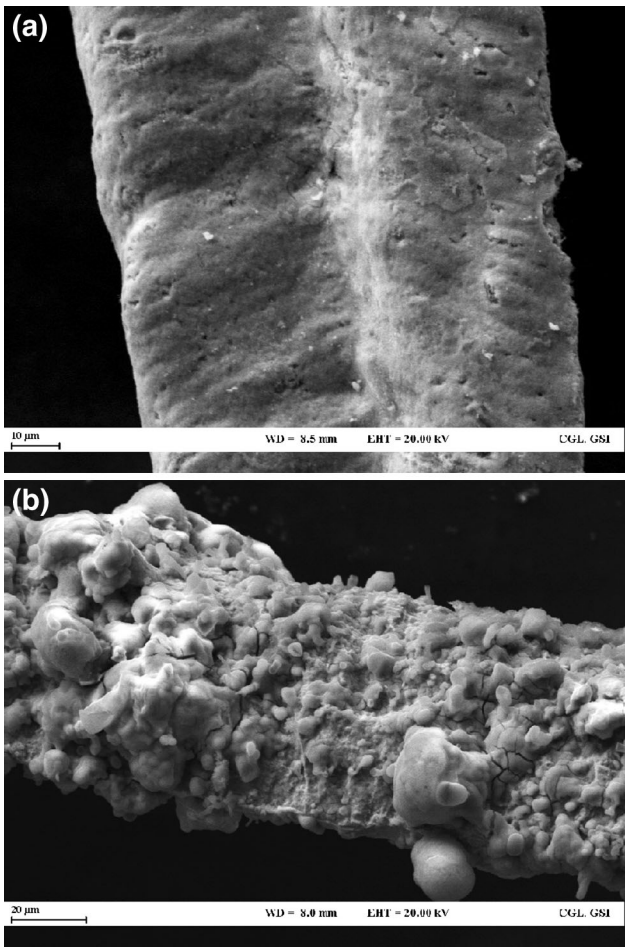

Fig. 2 SEM images for a single steel wool strand before (**a**) and after (**b**) reduction

parameters have to be determined as accurately as possible to validate the model. As the steel wool used in the present study was of commercial grade, the different geometric and physical properties of the same were determined by appropriate experiments, which are as follows.

The density of the steel wool sample was determined to be 8.25 g cm^{-3} using Micromeritics Accupyc II 1340 gas pycnometer with helium as analysis gas, a standard technique used by many researchers (Walker and Panozzo 2011; Dumee et al. 2012; Strubinger et al. 2012). The average radius of the unreacted steel wool was determined by processing the SEM image (Fig. 2a), off-line by Quantimet Quid-Pro Software, Leica, and an image analysis system, which operates under the same PC hardware. The average radius (R_0) was estimated to be 55 $\times$ 10^{-6} m. The length and external surface area of the hypothetical single strand, as used in the model formulation, equivalent to the actual multi-strand sample were calculated knowing the mass of the sample used for the experiments of transient response analysis of the Cr(VI)/Fe(0) system. The

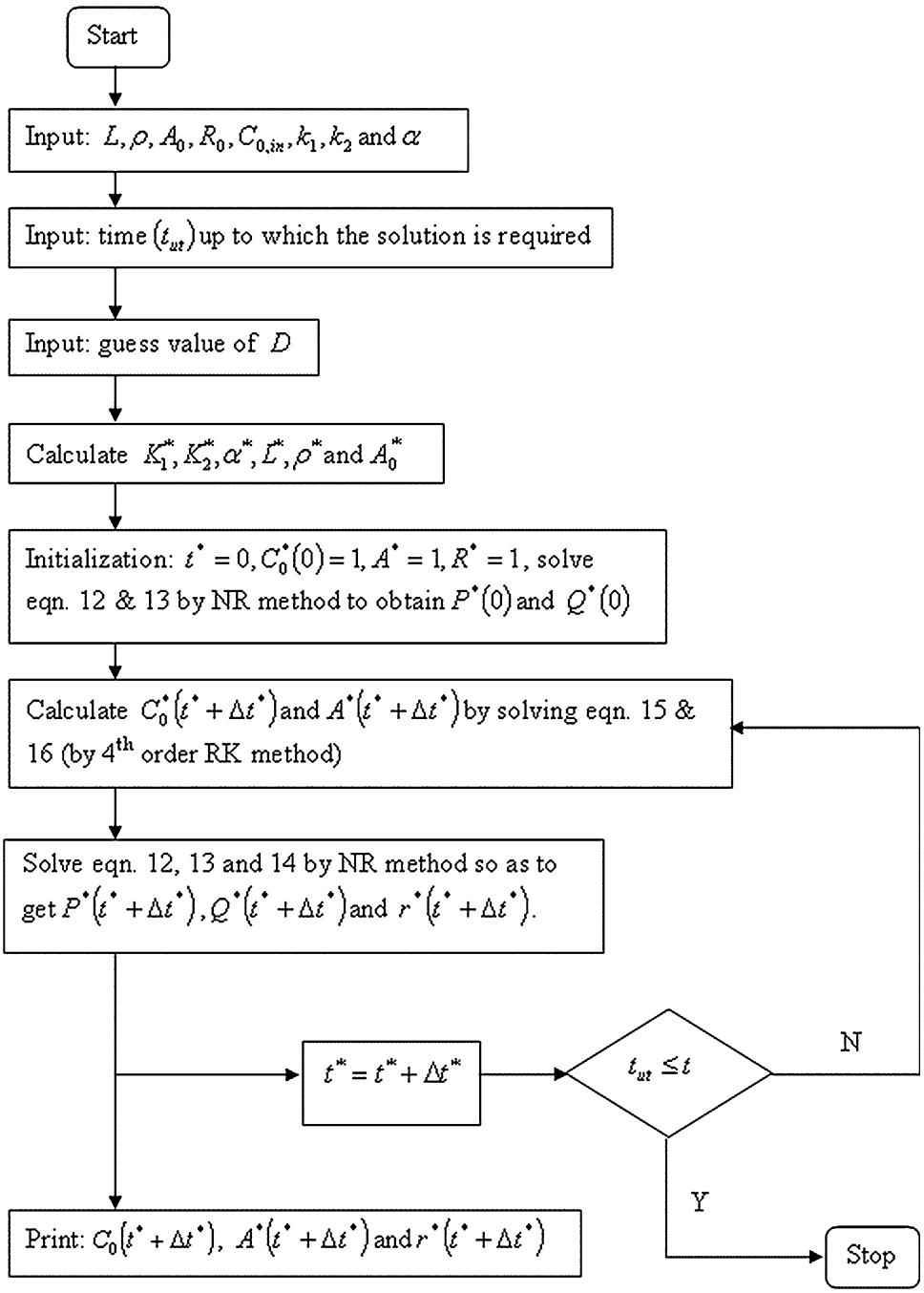

Fig. 3 Flow chart showing the algorithm for the simulation of transient bulk concentration, penetration depth and active external surface area

mass of the wool used was measured to be 0.3 g per batch. Knowing the density, L and A_0 were found to be 383 cm and 0.13 cm^2, respectively. As mentioned previously, the kinetic parameters, namely k_1, k_2 and α, were considered to remain same as that of our work on steel plate (Mitra et al. 2011). It is quite evident that any change of solid reactant's geometry only (from plate in the previous study to wool at present), in a solid–liquid reaction, without changing the chemical nature of the solid is not expected to alter the kinetic parameters of the corresponding reaction involved. So the values of k_1, k_2 and α were chosen to be 1.04×10^{-5} $mg^{1/3}$ $L^{-1/3}$ s^{-1} cm^{-2}, 2.69×10^{-5} cm^{-2} s^{-1} and 0.45 cm^2 L mg^{-1}, respectively. Once again, EDX data also indicate the iron content of the unreacted steel wool to be 93.2 wt%, which means $\phi_C = 0.932$. The only adjustable parameter D of the proposed model is determined by minimizing a global objective function $E(D)$ defined as follows (Sarkar et al. 2009)

$$E(D) = \frac{1}{5}\sum_{j=1}^{5}\sum_{i=1}^{m}\left(C_{0,ij}^{*\text{model}} - C_{0,ij}^{*\text{exp}}\right)^2 \quad (17)$$

where $C_{0,ij}^{*\text{exp}}$ and $C_{0,ij}^{*\text{model}}$ are the experimental and the model predicted dimensionless bulk concentrations at the particular time instant matching with ith experimental data point's time in the jth run. The total number of data points in a specific experimental run, characterized by a fixed initial bulk concentration is m. The objective function actually represents the average square error between the experimental data and the model predictions considering all the five different experimental runs marked by different initial bulk concentrations.

Simulation technique

The flowchart as shown in Fig. 3 depicts the algorithm for the simulation. It considers a single time loop for which the step size (Δt^*) is maintained to be 10^{-5} for all the runs. Since the analytical solution of the two simultaneous nonlinear ordinary differential equations, namely Eqs. (15) and (16) is impossible, the fourth order Runge–Kutta (RK) method is employed for solving the same in order to obtain $C_0^*(t^* + \Delta t^*)$ and $A^*(t^* + \Delta t^*)$, whereas standard multivariable Newton–Raphson (NR) method is used for solving Eqs. (12)–(14) so as to get $P^*(t^* + \Delta t^*)$, $Q^*(t^* + \Delta t^*)$ and $r^*(t^* + \Delta t^*)$.

With a chosen value of D, the algorithm is subjected to generate the transient bulk concentration profile for a specific initial bulk concentration. Subsequently, the objective function, $E(D)$ as described in Eq. (17) is calculated. In the next iteration, D value is changed to $D + \Delta D$ following the technique of single variable Fibonacci search (Beveridge and Schechter 1970) and the entire process is repeated unless the objective function $E(D)$ attains the desired minima.

Results and discussion

Reduction of hexavalent chromium by steel wool is facilitated by acidic pH. Extent of reduction after 120 min decreased very sharply from 30 to 9 % with increase in pH from 3 to 4 and remained at the same order of magnitude up to pH 8 (Fig. 4). We have carried out the experiments at pH 3. For the case of steel plate, the reduction was also carried out at the same pH. It is true that more acidic is the medium, better is the reduction. At the same time, the residual solution left after treatment becomes more acidic, this requires higher alkali dose to neutralize before finally discharged to the surface water. Total dissolved solid (TDS) loading will eventually be high enough in the treated water. Hence we have chosen the optimum pH to be 3. The speciation diagram in our previous work (Mitra et al. 2011) may be referred to for explanation of this influence of pH on the rate of reduction. Quite a few reports on the

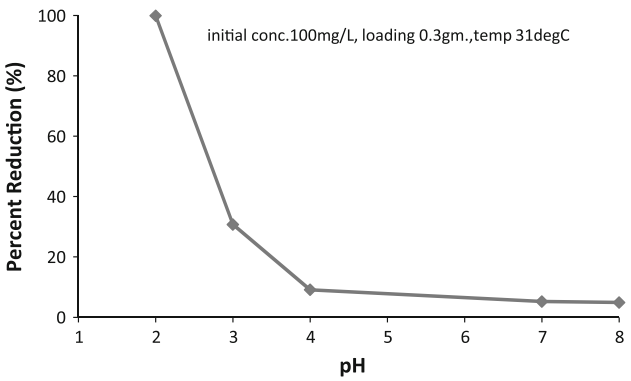

Fig. 4 Percent reduction of Cr(VI) vs. pH (experimental conditions: initial conc. 100 mg L^{-1}, loading 0.3 g and temperature 31 °C)

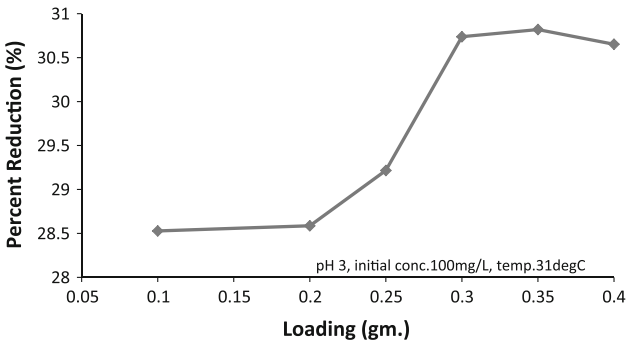

Fig. 5 Percent reduction of Cr(VI) vs. different loadings of steel wool (experimental conditions initial conc. 100 mg L^{-1}, pH 3 and temperature 31 °C)

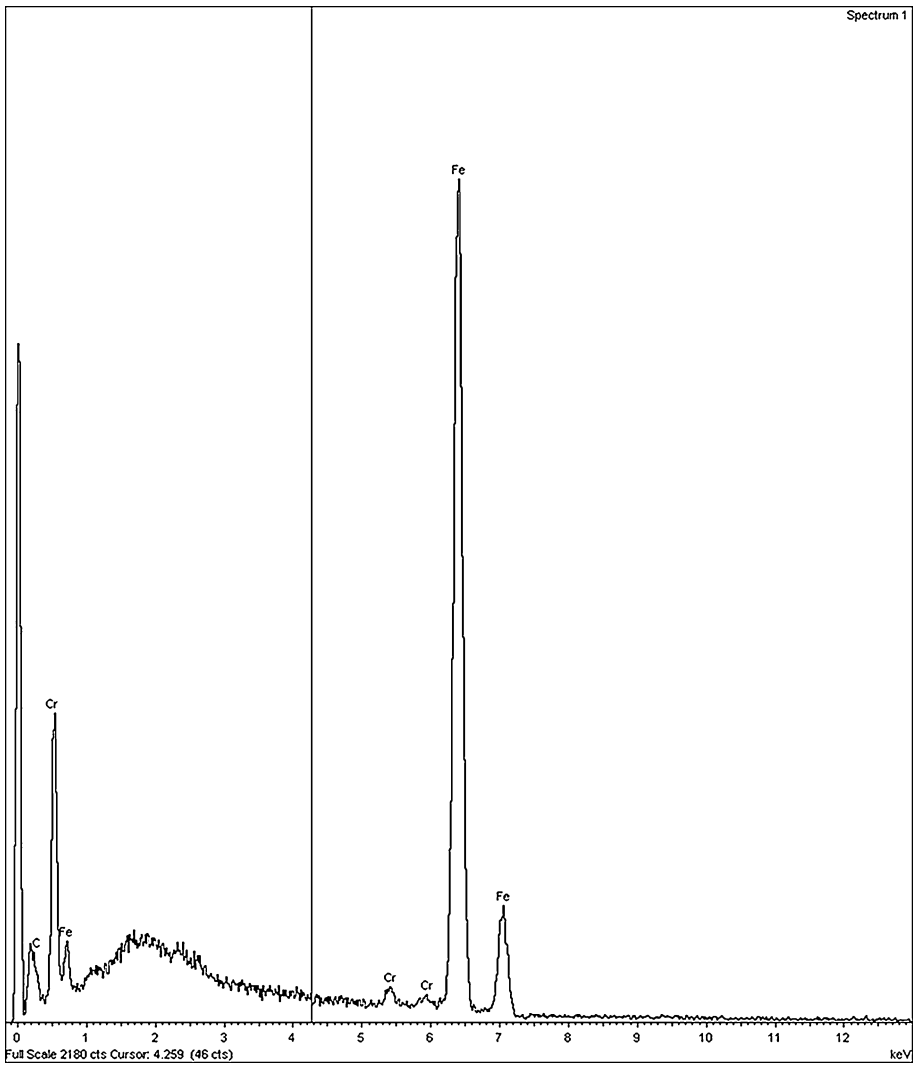

Fig. 6 EDX image showing various elements after reaction

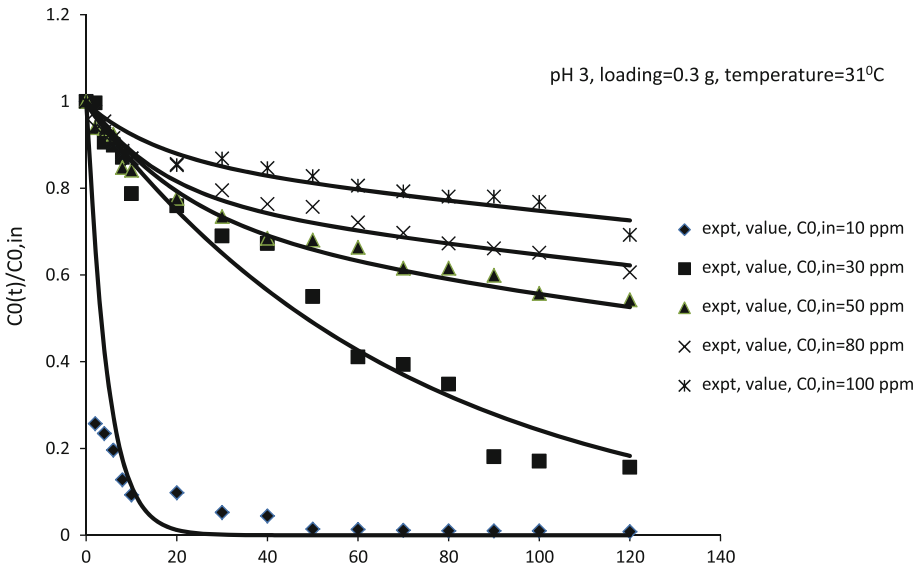

Fig. 7 Variation of the dimensionless concentration with time for five different initial concentrations of Cr(VI) under optimum parametric condition (pH 3, loading 0.3 g and temperature 31 °C)

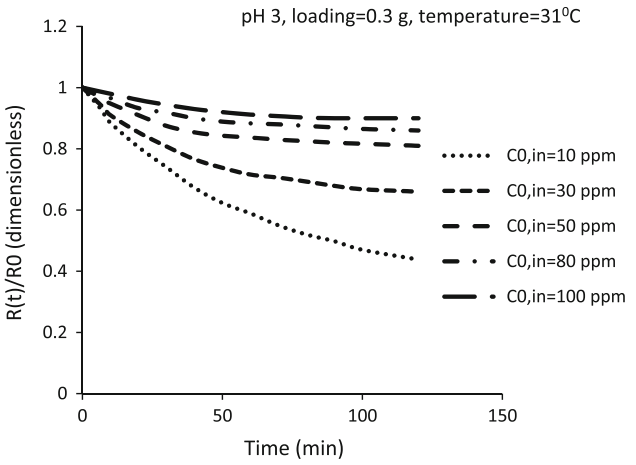

Fig. 8 Variation of dimensionless active unreacted core radius with time for five different initial concentrations of Cr(VI) under optimum parametric condition (pH 3, loading 0.3 g and temperature 31 °C)

thermodynamics of Cr(III)-H_2O and Fe(III)-H_2O systems over a wide pH range have been reported in the literature (Sass and Rai 1987; Eary and Rai 1988; Rai et al. 2004). Both the compounds exist in aqueous solutions in the form of several species including Cr^{3+}, $Cr(OH)^{2+}$, $Cr(OH)_2^+$, $Cr(OH)_3$ (Wilkin et al. 2005) and similar ones for Fe(III) in the acidic to neutral pH.

Loading of steel wool in 50 mL batches were varied from 0.1 to 0.4 g. Corresponding percent reduction after 120 min was observed to increase from 28 to 30 (Fig. 5). It may be noted that the change of percent reduction with the change in loading from 0.25 to 0.3 g was pretty high. However, the same was marginal when loading was changed from 0.3 to 0.35 g. Hence to keep the requirement of material to a minimum, especially important during scale-up, we have chosen the optimum loading to be 0.3 g for the present study.

Percent reduction after 120 min increased uniformly from 30 to 67 with increase in temperature from 304 to 336 K under otherwise same experimental conditions; however, for the experimental convenience, the experiments have been undertaken at 304 K (31 °C).

As in case of steel plates, the reduction after 120 min decreased from 84 to 36 % as the initial substrate concentration increased from 10 to 100 mg L^{-1}. The observation is supported by a few reports and a detailed discussion on the passive layer formed on the surface has been provided in our work with steel plate (Mitra et al. 2011). SEM images (Fig. 2a, b) for a single steel wool strand before and after reduction show the formation of passive layer also on the surface of steel wool. It is also observed that there is no decrease in diameter. EDX analysis (Fig. 6) indicates peak of chromium on the used steel wool surface, and there was a decrease in iron content from 93 to 74 wt% on the surface after reaction (Table not shown).

To obtain the dimensionless transient bulk concentration $\left(C_0^* = \frac{C_0(t)}{C_{0,\text{in}}}\right)$ against time, Eqs. (12)–(16) are solved with the simultaneous global optimization of the parameter D following the algorithm as described in Fig. 3. The simulated results have been compared with the experimental data at five different initial bulk concentration of Cr(VI) ($C_{0,\text{in}} = 10, 30, 50, 80, 100$ mg L^{-1}) at pH 3 with a steel wool loading of 0.3 g is depicted in Fig. 7.

The figure clearly indicates that the model prediction agree reasonably well with the experimental data. The maximum standard deviation for all the five different initial concentrations was found to be 0.09. This explains the

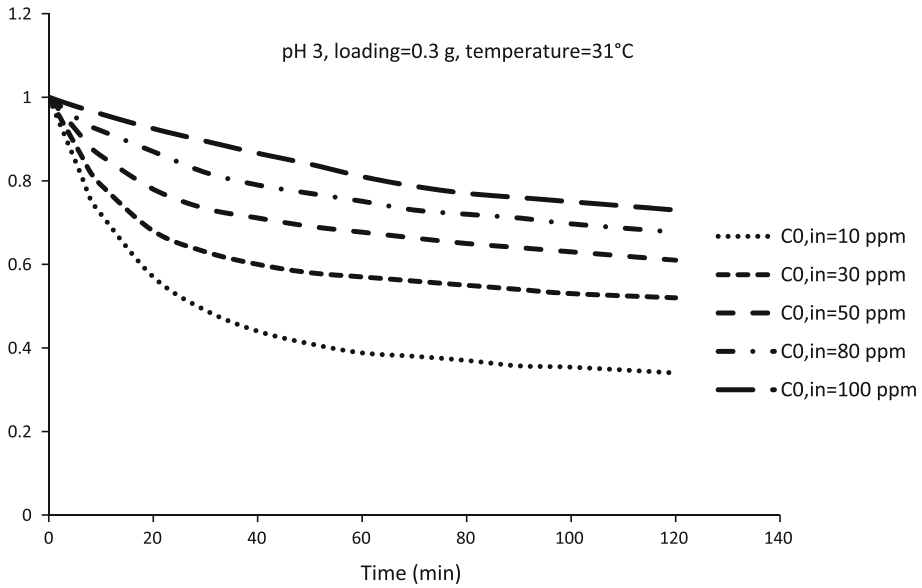

Fig. 9 Variation of dimensionless active external surface area of steel wool with time for five different initial concentrations of Cr(VI) under optimum parametric condition (pH 3, loading 0.3 g and temperature 31 °C)

general validity of the proposed model in describing the reduction of Cr(VI) in aqueous medium by commercial steel wool. The only adjustable parameter of the proposed model, namely the diffusivity of Cr(VI) in the external product layer (D) leading to the closest match between the experimental data for all the five different initial concentrations and the corresponding model predictions was determined by minimizing the global objective function, $E(D)$. The optimum D value was found to be 0.08 $cm^2\ s^{-1}$. The shrinkage rate of the unreacted core, predicted by the proposed model is also reported by plotting dimensionless radius, r^* with time as shown in Fig. 8.

The maximum steady state penetration (i.e., penetration at $t = 120$ min), in terms of $\frac{R(t)}{R_0}$ was close to 0.44 for $C_{0,in} = 10\ mg\ L^{-1}$. The decline of active external surface area, in dimensionless form $A^*(t)$ with time is shown in Fig. 9. The rate of reduction of transient external surface area was considered to be proportional to the rate of passivation, which was assumed to be restricted over the external surface area of the wool following a first order kinetics.

The constant of proportionality (α) at pH 3, as reported in our previous study of Cr(VI) reduction using steel plate (Mitra et al. 2011), was considered to remain unchanged. Compared to the case of steel plate, the degree of passivation $[= (1 - A^*) \times 100\,\%]$ was found to be reduced in the present study. For example, at $C_{0,in} = 50\ mg\ L^{-1}$, the passivated surface area at $t = 60$ min was 74 % of the total external surface area for steel plate, where the same was only 34 % for steel wool. This may be attributed to the curvature effect of steel wool. According to the well-known Kelvin equation (Adamson and Gast 1997), the local concentration of Cr(VI), close to the solid–liquid interface, decreases due to the negative curvature of the interface as seen from the liquid side. Similar observation for nanostructure material has been reported in literature (Ouyang et al. 2009). On the other hand, as the rate of passivation reaction $\left[= \left(-\frac{dC}{dt}\right)_2\right]$, to which area blockage rate $\left(= -\frac{dA}{dt}\right)$ is proportional, is a monotonically increasing function of local Cr(VI) concentration, it is expected that degree of passivation in case of wool would be less compared to that of the plate.

Conclusion

The present batch kinetic study clearly advocates for the effectiveness of commercial steel wool, which is mostly Fe(0), as a reducing agent for chromium remediation in wastewater. A moving boundary type kinetic model has been proposed and validated using the transient bulk concentration data obtained under optimum pH and loading condition. The proposed model incorporates the effects of passivation in the overall uptake of Cr(VI) from aqueous phase in addition to the primary redox reaction. The only adjustable parameter of the model, namely, the effective diffusivity of Cr(VI) in steel wool has been evaluated using a suitable global optimization technique. In addition to the transient bulk concentration and the degree of penetration of Cr(VI), the external surface area blockage rate of the steel wool caused by passivation was also simulated. Compared to our previous study of Cr(VI)/Fe(0) system with steel plates, passivation-induced degree of external area blockage was much lower in case of steel wool. Accordingly, it may be concluded that low-cost commercial steel wool may serve as an effective reducing agent in the treatment of chromium-contaminated wastewater in general.

Acknowledgments UGC Major Research Project F. No. 34-395/2008 (SR) dated 26.12.2008. Bose Institute, Kolkata for EDX. Prof. B. K. Dutta, Chairman, WBPCB. Mr. Dipankar Chakrabarti.

Nomenclature

$A(t)$	Transient active surface area of Fe(0) plate (cm^2)
A_0	Initial surface area of Fe(0) plate (cm^2)
A^*	Dimensionless transient active surface area of Fe(0) plate (dimensionless)
$C(t)$	Transient bulk concentration of Cr(VI) in aqueous phase ($mg\ L^{-1}$)
C_0	Initial bulk concentration of Cr(VI) ($mg\ L^{-1}$)
C_0^*	Dimensionless transient bulk concentration of Cr(VI) in aqueous phase (dimensionless)
$C_{ij}^{*\,exp}$	Dimensionless ith experimental data of transient aqueous phase bulk concentration of Cr(VI) in jth experimental run (dimensionless)
C_{ij}^{*model}	Dimensionless model predicted transient aqueous phase bulk concentration of Cr(VI) at time same as that of ith experimental data of jth experimental run (dimensionless)
D	Effective diffusivity of Cr(VI) in steel wool ($cm^2\ s^{-1}$)
E	Global objective function as described in Eq. (17) (dimensionless)
k_1	Rate constant of primary redox reaction ($mg^{1/3}\ L^{-1/3}\ s^{-1}\ cm^{-2}$)
k_2	Rate constant of passivation reaction ($s^{-1}\ cm^{-2}$)
K_1^*	Dimensionless constant as described in Eq. (15) (dimensionless)
K_2^*	Dimensionless constant as described in Eq. (16) (dimensionless)
L	Equivalent length of steel wool (cm)

L^*	Dimensionless equivalent length of steel wool (dimensionless)
P	Parameter defined in Eq. (4) (mg L^{-1})
P^*	Parameter defined in Eq. (12) (dimensionless)
Q	Parameter defined in Eq. (4) (mg L^{-1})
Q^*	Parameter defined in Eq. (12) (dimensionless)
r	Radial coordinate (cm)
r^*	Dimensionless radius of the virgin core of the steel wool (dimensionless)
$R(t)$	Radius of the virgin core of the steel wool (cm)
R_0	Radius of the steel wool (cm)
$R_{\mathrm{Cr(VI)}}\big\vert_1$	Uptake rate of Cr(VI) via the primary redox reaction route at the interface between virgin core and product layer of steel wool (mg cm s^{-1} L^{-1})
t	Time (s)
t^*	Dimensionless time (dimensionless)
α	Proportionality constant as described in Eq. (11) (cm^2 L mg^{-1})
α^*	Dimensionless constant as described in Eq. (16) (dimensionless)
ρ	Density of the steel wool (mg L^{-1})
ρ^*	Dimensionless density of the steel wool (dimensionless)
φ_C	Weight fraction of Fe(0) in steel wool (dimensionless)

References

Adamson AW, Gast AP (1997) Physical chemistry of surfaces, 6th edn. Wiley, New York

Agrawal A, Kumar V, Pandey BD (2006) Remediation options for the treatment of electroplating and leather tanning effluent containing chromium—a review. Miner Process Extract Metall Rev 27(2):99–130

Beveridge SG, Schechter RS (1970) Optimization: theory and practice. McGraw-Hill, Inc., New York

Blowes DW, Gillham RW, Ptacek CJ, Puls RW, Benett TA, O'Hannesin SF, Hanton-Fong CJ, Bain JG (1996) An in situ permeable reactive barrier for the treatment of hexavalent chromium and trichloroethylene in ground water. design and installation, vol. 1, United States Environmental Protection Agency

Blowes DW, Ptacek CJ, Benner SG, McRae C, Bennett TA, Puls RW (2000) Treatment of inorganic contaminants using permeable reactive barriers. J Contam Hydrol 45(1–2):123–137

Botta SG, Navio JA, Hidalgo MC, Restrepo GM, Litter MI (1999) Photocatalytic properties of ZrO_2 and Fe/ZrO_2 semiconductors prepared by a sol-gel technique. J Photochem Photobiol A 129(1–2):89–99

Bowers AR, Huang CP (1980) Activated carbon process for treatment of automotive application for chromium wastewaters containing hexavalent chromium. Prog Water Technol 12(1):629–634

Cantrell KJ, Kaplan DI, Wietsma TW (1995) Zero-valent iron for the in situ remediation of selected metals in groundwater. J Hazard Mater 42(2):201–212

Cheryl P, Susan MB (2000) Reflections of hexavalent chromium: health hazards of an industrial heavyweight. Environ Health Perspect 108(9):48–58

Coelho FS, Ardisson JD, Moura FCC, Lago RM, Murad E, Fabris JD (2008) Potential application of highly reactive Fe(0)/Fe_3O_4 composites for the reduction of Cr(VI) environmental contaminants. Chemosphere 71(1):90–96

Dumee L, Hill MR, Duke M, Velleman L, Sears K, Schütz J, Finn K, Gray S (2012) Activation of gold decorated carbon nanotube hybrids for targeted gas adsorption and enhanced catalytic oxidation. J Mater Chem 22(24):9374–9378

Dutta R, Mohammad S, Chakrabarti S, Chaudhuri B, Bhattacharjee S, Dutta BK (2010) Reduction of hexavalent chromium in aqueous medium with zerovalent iron. Water Environ Res 82(2):138–146

Eary LE, Rai D (1988) Chromate removal from aqueous wastes by reduction with ferrous ion. Environ Sci Technol 22(8):972–977

El-Shazly AH, Mubarak AA, Konsowa AH (2005) Hexavalent chromium reduction using a fixed bed of scrap bearing iron spheres. Desalination 185(1–3):307–316

Fiúza A, Silva A, Carvalho G, de la Fuente AV, Delerue-Matos C (2010) Heterogeneous kinetics of the reduction of chromium (VI) by elemental iron. J Hazard Mater 175(1):1042–1047

Goeringer S, Chenthamarakshan CR, Rajeswar K (2001) Synergistic photocatalysis mediated by TiO_2: mutual rate enhancement in the photoreduction of Cr(VI) and Cu(II) in aqueous media. Electrochem Commun 3(6):290–292

Gómez-Barea A, Ollero P (2006) An approximate method for solving gas–solid non-catalytic reactions. Chem Eng Sci 61(11):3725–3735

Gould JP (1982) The kinetics of hexavalent chromium reduction by metallic iron. Water Res 16(6):871–877

He YT, Traina SJ (2005) Cr(VI) Reduction and immobilization by magnetite under alkaline pH conditions: the role of passivation. Environ Sci Technol 39(12):4499–4504

Katz SA, Salem H (1992) The toxicology of Cr with respect to speciation: a review. J Appl Toxicol 13(3):217–224

Kogel JE, Trivedi NC, Barker JM, Krukowski ST (2006) Industrial minerals and rocks, 7th edn. Society for Mining, Metallurgy and Exploration (SME), Colorado

Ku Y, Jung I (2001) Photocatalytic reduction of Cr(VI) in aqueous solutions by UV irradiation with the presence of titanium dioxide. Water Res 35(1):135–142

Kulkarni PS, Kalyani V, Mahajani VV (2007) Removal of hexavalent chromium by membrane-based hybrid processes. Ind Eng Chem Res 46(24):8176–8182

Levenspeil O (1998) Chemical reaction engineering, 3rd edn. Wiley, New York

Melitas N, Chuffe-Moscoso O, Farrell J (2001) Kinetics of soluble chromium removal from contaminated water by zerovalent iron media: corrosion inhibition and passive oxide effects. Environ Sci Technol 35(19):3948–3953

Mitra P, Sarkar D, Chakrabarti S, Dutta BK (2011) Reduction of hexa-valent chromium with zero-valent iron: batch kinetic studies and rate model. Chem Eng J 171(1):54–60

Navio JA, Testa JJ, Djedjeian P, Padron JR, Rodriguez D, Litter MI (1999) Iron-doped titania powder prepared by a sol-gel method. Part II: Photocatalytic properties. Appl Catal A 178(2):191–203

Ouyang G, Wang CX, Yang GW (2009) Surface energy of nanostructural materials with negative curvature and related size effects. Chem Rev 109(9):4221–4247

Özer A, Altundoğan HS, Erdem M, Tümen F (1997) A study on the Cr(VI) removal from aqueous solutions by steel wool. Environ Pollut 97(1–2):107–112

Patisson F, François MG, Ablitzer D (1998) A non-isothermal, non-equimolar transient kinetic model for gas-solid reactions. Chem Eng Sci 53(4):697–708

Puls RW, Blowe DW, Gillham RW (1999) Long term performance monitoring of a permeable reactive barrier at the US Coast Guard Support Center, Elizabeth City, North Carolina. J Hazar Mater 68(1–2):109–124

Rai D, Moore DA, Hess NJ, Rao L, Clark SB (2004) Chromium (III) hydroxide solubility in the aqueous Na^{+}-OH–H_2PO_4–HPO_4^{2}–PO_4^{3}–H_2O System: a Thermodynamic Model. J Solut Chem 33(10):1213–1242

Rivero-Huguet M, Marshall WD (2009) Reduction of hexavalent chromium mediated by micro- and nano-sized mixed metallic particles. J Hazard Mater 169(1–3):1081–1087

Sarkar D, Chakrabarti S, Dutta BK (2009) Diffusion of mythelene blue in glass fibers-Application of shrinking core model. Appl Math Model 33(6):2874–2881

Sass BM, Rai D (1987) Solubility of Amorphous Chromium (III)–Iron (III) hydroxide solid solutions. Inorg Chem 26(14):2228–2232

Song D, Kim YH, Shin WS (2005) A simple mathematical analysis on the effect of sand in Cr(VI) reduction using zero valent iron. Korean J Chem Eng 22(1):67–69

Strubinger A, Ehrmann U, León V (2012) Using the gas pycnometer to determine API gravity in crude oils and blends. Energy Fuels 26(11):6863–6868

Walker CK, Panozzo JF (2011) Development of a small scale method to determine volume and density of individual barley kernels, and the relationship between grain density and endosperm hardness. J Cereal Sci 54(3):311–316

Wang XS, Tang YJ, Chen LF, Li FY, Wan WY, Tan YB (2010) Removal of Cr(VI) by zero-valent, iron-encapsulated alginate beads. Clean Soil Air Water 38(3):263–267

Wilkin RT, Su C, Ford RG, Paul CJ (2005) Chromium removal processes during groundwater remediation by zero-valent iron permeable reactive barrier. Environ Sci Technol 39(12):4599–4605

Williams AGB, Scherer MM (2001) Kinetics of Cr(VI) reduction by carbonate green rust. Environ Sci Technol 35(17):3488–3494